

Controllable Morphology and Structure of MoO₃ Hexagonal Poles and Nanobelts†

QINGCHUN ZHAO* and TIAN CAO

Department of Material Science and Engineering, Anhui Institute of Architecture and Industry, Hefei, Anhui Province, P.R. China

*Corresponding author: E-mail: qczhao@ustc.edu

AJC-13246

Various morphology and structure of MoO₃ were prepared *via* hydrothermal reaction method. The experimental results show that Na⁺ and H⁺ play a decisive role in the formation of *h*-MoO₃ and α-MoO₃. As mol ratio of Na₂MoO₄ : H₂SO₄ = 1 : 2 and 1, α-MoO₃ nanobelts and *h*-MoO₃ hexagonal poles were obtained, respectively. Scanning electron microscopy and transmission electron microscopy images of the products clearly show that MoO₃ possesses a nanobelt and hexagonal pole structure. Electron diffraction patterns of MoO₃ nanobelt and hexagonal pole, Raman spectra and X-ray diffraction analysis were used to examine the crystal structure of the obtained products. The obtained nanobelts are pure-phase orthorhombic α-MoO₃ nanobelts and hexagonal poles are pure-phase metastable phase of hexagonal *h*-MoO₃.

Key Words: Controllable morphology, MoO₃, Hexagonal poles, Nanobelts.

INTRODUCTION

The synthesis of inorganic materials with controllable morphology and structure on the nanometer scale has greatly improved in the last 20 years¹⁻⁷. Various shape nanostructures, such as nanorods, nanowires, nanobelts and nanotubes, are known to have many fascinating physical and chemical properties and are of great importance in both basic scientific research and potential technological applications⁸. Many unique and interesting properties have been proposed or demonstrated for nanoscale materials, such as superior mechanic toughness, higher luminescence efficiency, enhancement of thermoelectric figure of merit and lowered lasing threshold⁹⁻¹¹.

Molybdenum trioxide (MoO₃) is not only one of the most important catalysts in modern industry^{12,13}, but also it is a promising material in photochromic and electrochromic devices^{14,15}, sensors¹⁶, lithium battery¹⁷ and hydrogen absorption¹⁸. In the past few years, remarkable progress has been achieved concerning the preparation of various shape molybdenum oxide, such as molybdenum oxide fibers¹⁹, nanotubes²⁰, nanobelts²¹, hexagonal nanoplates²², hollow MoO₃ nanospheres²³, branched and flower-like *r*-MoO₃ nanobelt arrays²⁴ and mesostructured molybdenum oxide toroids²⁵.

Herein, we report a hydrothermal method developed to prepare high-quality *h*-MoO₃ hexagonal poles and α-MoO₃ nanobelts. In the present reaction system, the existence of OP X-100 and different mol ratio of Na₂MoO₄ : H₂SO₄ are proved to influence morphology and structure of the obtained MoO₃.

EXPERIMENTAL

Controlled growth MoO₃ nanobelts and hexagonal poles: The controlled growth MoO₃ nanobelts and hexagonal poles were based on a hydrothermal method. In a typical procedure, 1.215 g (0.005 mol) Na₂MoO₄·2H₂O used as the precursor and 0.6258 g of OP10 and different mol amount H₂SO₄ were added into 60 g water. After 10 min of stirring, 30 g mixture was sealed in an autoclave, heated at 180 °C for 12 h. Then the autoclave was allowed to cool to room temperature naturally. The solid phase was centrifuged at 16000 rpm for 2 min. The final product was collected by washed with deionized water to remove any possible ionic remnants and OP 10 residue and then dried at 60 °C for 24 h.

RESULTS AND DISCUSSION

X-ray powder diffraction: The *h*-MoO₃ hexagonal poles were obtained *via* MoO₄²⁻ ions reaction with H⁺. The phase and crystallographic structure of the MoO₃ products were investigated using powder XRD technique. Fig. 1a shows the XRD pattern of as-synthesized hexagonal poles, which is in good agreement with the hexagonal *h*-MoO₃ phase with lattice parameters of *a* = 10.53 Å and *c* = 14.87 Å (JCPDS card No. 21-0569, space group P63). No other phases are detected in final products. In the XRD pattern, the strong diffraction peaks of (020), (040) and (060) relative to other planes indicates that most hexagonal poles lie on the holder with {010} planes and they have the preferential growth in the [010] direction.

†Presented to the 6th China-Korea International Conference on Multi-functional Materials and Application, 22-24 November 2012, Daejeon, Korea

The XRD pattern of MoO₃ nanobelts is demonstrated in Fig. 1b. All diffraction peaks can be exclusively indexed as the orthorhombic MoO₃ phase (commonly denoted as α -MoO₃) with lattice parameters of $a = 0.3963$ nm, $b = 1.3856$ nm and $c = 0.3697$ nm and a space group of $Pbnm$, slightly bigger than those presented in JCPDS No. 35-0609). Suggesting a high purity of the α -MoO₃ nanobelts were obtained.

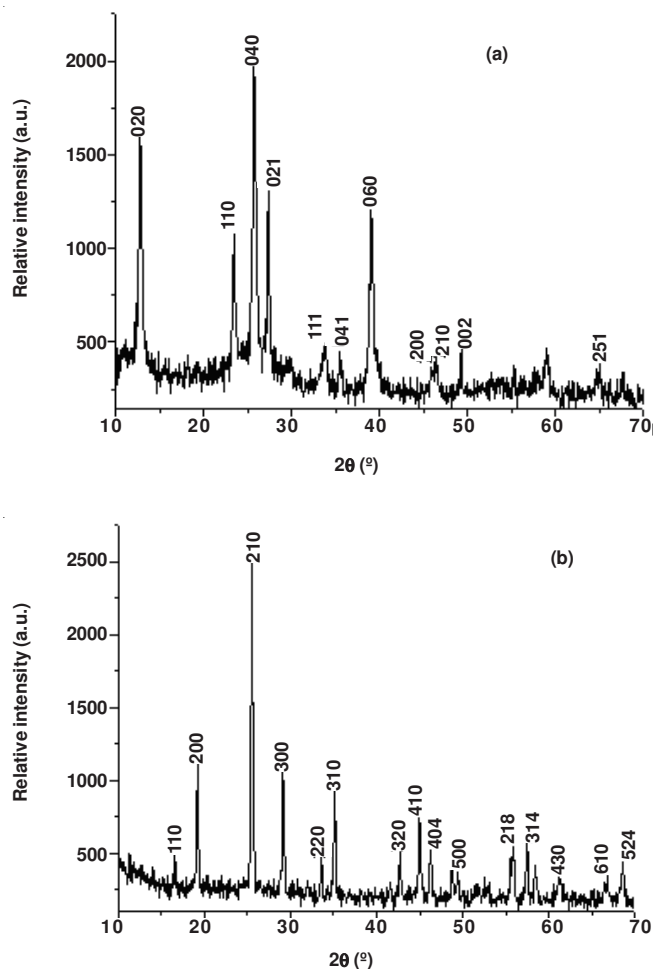


Fig. 1. XRD pattern of the as-synthesized MoO₃ nanostructures. a and b are the XRD pattern of obtained h -MoO₃ hexagonal poles and α -MoO₃ nanobelts, respectively

Scanning electron microscopy and transmission electron microscopy: The product morphology was determined by scanning electron microscopy. Fig. 2a is a typical SEM image of the obtained α -MoO₃ nanobelts, clearly showing that MoO₃ possesses a belt structure. Experimental result indicates that the well-defined MoO₃ nanobelts can be obtained under the present experimental conditions. A higher magnification SEM image clearly shows their belt structure, as demonstrated in Fig. 2b. The length, width and the thickness of the MoO₃ nanobelts are about several micron, 80-200 nm and 20-30 nm, respectively.

Fig. 2c is a typical SEM image of the obtained MoO₃ hexagonal poles. From this image, we can see that all MoO₃ poles possess an hexagonal pole structure. Examining numerous SEM images of the sample prepared at 180 °C for 12 h and mol ratio of Na₂MoO₄ : H₂SO₄ = 1:1. Experimental result

indicates that well-defined h -MoO₃ hexagonal poles can be obtained under the present experimental conditions. Fig. 2d is the high magnification image of hexagonal poles.

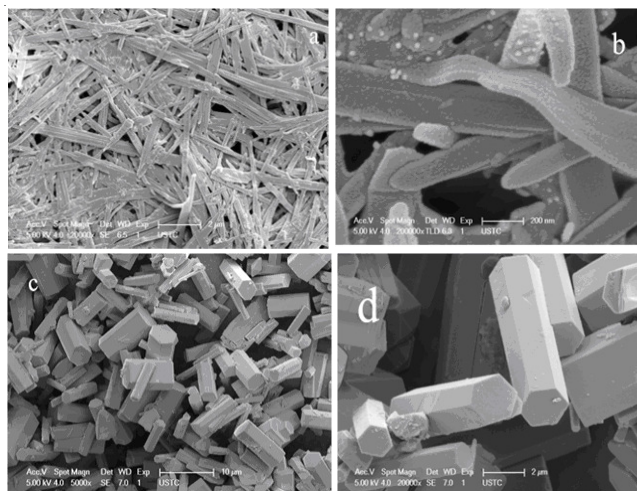


Fig. 2. a, b are SEM images of MoO₃ nanobelts. c, d are SEM images of MoO₃ hexagonal poles

The obtained products were further characterized by transmission electron microscopy. A typical TEM image is shown in Fig. 3a, indicating that the α -MoO₃ nanobelts are indeed observed. From the picture, we can see that the TEM image is nearly transparent (Fig. 3a). It indicates that the α -MoO₃ nanobelts thickness is thin and possess a large surface area. Fig. 3b reveals the TEM image of an individual nanobelt and its corresponding HRTEM and SAED patterns are shown in Fig. 3c, respectively. Electron diffraction patterns (inset b) taken from a single MoO₃ nanobelts reveal the single-crystalline nature of the sample and can be indexed as the c -axis of the orthorhombic MoO₃. The ED pattern can be indexed as a orthorhombic phase and grown along the [001] direction. Two sets of crystal lattice fringes, corresponding to the {100} (0.397 nm) and {001} (0.369 nm) atomic spacings, can be clearly distinguished in the top-view high-resolution, which is consistent with the XRD results.

TEM images of an individual h -MoO₃ hexagonal pole and its corresponding HRTEM and SAED patterns are shown in Fig. 3e-g, respectively. A striking feature of the h -MoO₃ hexagonal poles is that they are apt to recrystallize under the electron irradiation (Fig. 3f). The corresponding SAED pattern presents several faint spots with vague halo rings, where the spots indexed into the (100) and (001) planes are also typical electron diffraction spots as reported results in previous literature. From HRTEM images the (110) interplanar spacings were derived to be 0.525 nm. It is reasonable that the h -MoO₃ hexagonal poles lose the crystalline state under the electron irradiation and a similar phenomenon has been observed on metastable hexagonal phase nanobelts.

Raman spectrum: Room temperature Raman spectrum for obtained nanobelts and hexagonal poles are shown in Fig. 4, respectively. Fig. 4a is Raman spectrum for obtained nanobelts. From Fig. 4a, we can see the peak positions are at 128, 155, 242, 288, 336, 375, 459, 664, 821 and 994 cm⁻¹, which agree well with those reported by Pan *et al.*¹² and Chen *et al.*²². The

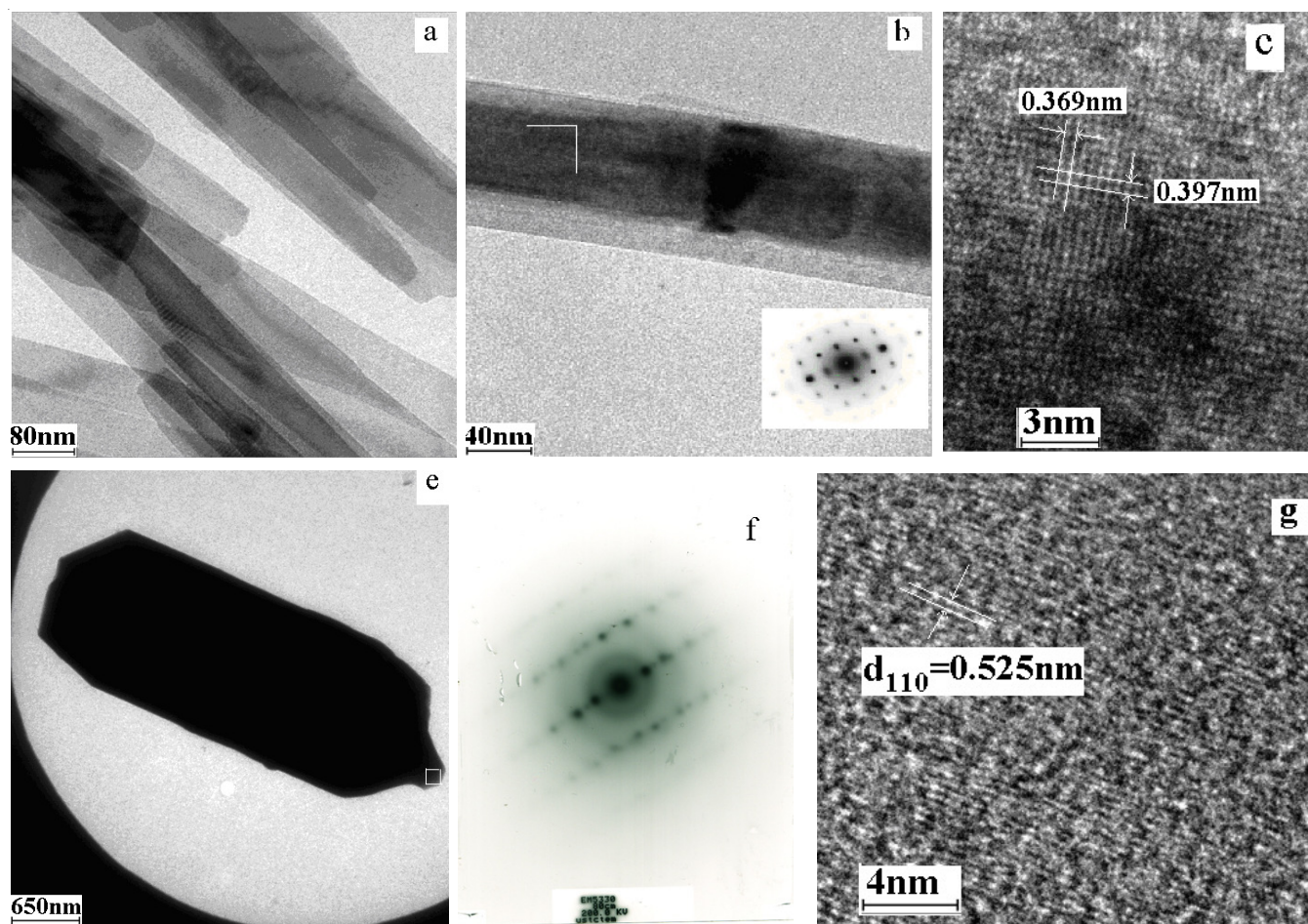


Fig. 3. From a to c TEM images of α -MoO₃ nanobelts. b) an individual α -MoO₃ nanobelt, insert is electron diffraction patterns. c) its HRTEM image; From e to g TEM images of h -MoO₃ hexagonal poles. f) is electron diffraction patterns; g) individual MoO₃ hexagonal pole HRTEM image

irreducible representation of MoO₃ with space group D_{2h}¹⁶ (*Pbnm*) is given as follows:

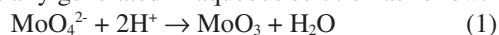
$$\Gamma = 8A_g + 8B_{1g} + 4B_{2g} + 4B_{3g} + 4A_u + 3B_{1u} + 7B_{2u} + 7B_{3u}$$

where A_g, B_{1g}, B_{2g} and B_{3g} are Raman-active modes.

This result suggests the better crystallinity of the obtained α -MoO₃ nanobelts, being consistent with the XRD results. No corresponding peaks in position were observed for h -MoO₃. It is obvious that the frequencies of the spectrum display a red shift of about 1–7 cm⁻¹. The decrease in the Raman frequencies may be attributed to the nanosize of our single crystals²². The calculations of the valence force field downward frequency shifts point to a reduction of interaction between layers and chains, which contributes to the perturbation in the layered structure²⁶, which is consistent with the XRD results.

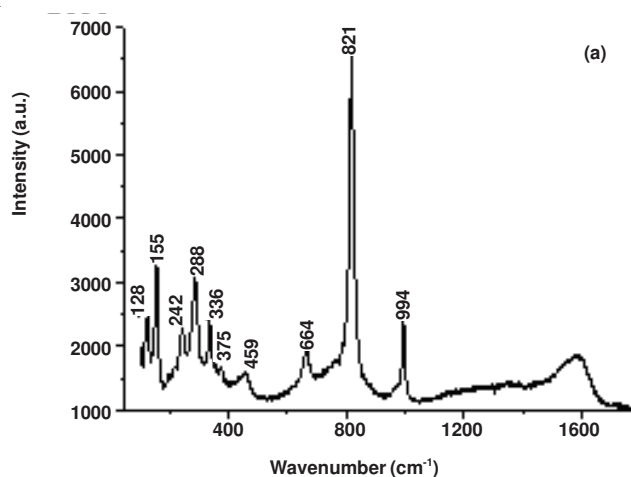
Fig. 4b clearly shows Raman spectrum for obtained hexagonal poles. The peaks at 688, 879, 899 and 976 cm⁻¹ tend to move toward the side of lower bands.

Our method is based on treating the Na₂MoO₄ precursor in the presence of H₂SO₄ under hydrothermal conditions. When solution was sealed in an autoclave, heated to 180 °C for 12 h, the reactions could sequentially occur in the reaction system. MoO₃ was initially generated in aqueous solution as follow:



A control experiment demonstrated that hydrothermal reaction with different mol ratio of Na₂MoO₄ : H₂SO₄, obtained different structure MoO₃, suggesting that Na⁺ and H⁺ play a

decisive role in the formation of h -MoO₃ and α -MoO₃. As mol ratio of Na₂MoO₄ : H₂SO₄ = 1:2, being large number of H⁺ ions in solution, H⁺ play a decisive role in the formation of α -MoO₃¹². MoO₆ octahedra readily share two vertices at the para position, so that zigzag chains connect *via* an oxolation mode to produce layers in MoO₃ stoichiometry. These layers are stacked in a staggered arrangement and are only held together by weak van der Waals forces to produce a three dimensional framework of α -MoO₃.



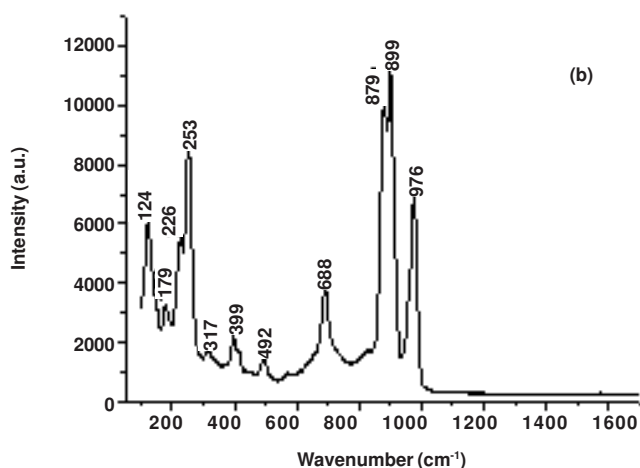


Fig. 4. a,b are Raman spectra of α -MoO₃ nanobelts and h -MoO₃ hexagonal poles, respectively

Nevertheless, as mol ratio of Na₂MoO₄ : H₂SO₄ = 1:1, being large number of Na⁺ ions in solution, Na⁺ play a decisive role in the formation of h -MoO₃. The existence of Na⁺ may change the oxolation mode because of the electrostatic interaction existing between Na⁺ and oxygen atom²¹. For more oxygen atoms interacting with Na⁺, [MoO₆] octahedra share two vertexes at the *ortho*-position and thus zigzag chains interlink each other through the *cis*-position, leading to the spontaneous arrangement of hexagonal crystalline structure with large one-dimensional tunnels.

Conclusion

In summary, we have presented a simple hydrothermal process for preparing controlable morphology and structure of MoO₃ materials. The experimental results show Na⁺ and H⁺ play a decisive role in the formation of h -MoO₃ hexagonal poles and α -MoO₃ nanobelts. Our study may provide a effectively method for controlable growth of various morphology and structure related nanostructure materials.

REFERENCES

1. C.B. Murray and D.J. Norris, *J. Am. Chem. Soc.*, **115**, 8706 (1993).
2. J.T. Hu, T.W. Odom and C.M. Lieber, *Acc. Chem. Res.*, **32**, 435 (1999).
3. K. Chung, C. Lee and G. Yi, *Science*, **29**, 655 (2010).
4. X.Y. Kong, Y. Ding, R. Yang and Z.L. Wang, *Science*, **27**, 1348 (2004).
5. Y. Wu and P. Yang, *J. Am. Chem. Soc.*, **123**, 3165 (2001).
6. Z.A. Peng and X. Peng, *J. Am. Chem. Soc.*, **124**, 3343 (2002).
7. C.J. Murphy and N.R. Jana, *Adv. Mater.*, **14**, 80 (2002).
8. G. Patzke and R.F. Krumeich, *Angew. Chem. Int. Ed.*, **41**, 2446 (2002).
9. X.F. Duan, Y. Huang, J.F. Wang and C.M. Lieber, *Nature*, **409**, 66 (2001).
10. Z.W. Pan and Z.Z.L. Wang, *Science*, **9**, 1947 (2001).
11. P.X. Gao, Y. Ding, W.J. Mai, W.L. Hughes, C. Lao and Z.L. Wang, *Science*, **9**, 1700 (2005).
12. W. Pan, R. Tian, H. Jin, Y. Guo and L. Zhang, *Chem. Mater.*, **22**, 6202 (2010).
13. N. Al-Yassir and V. Le, *Appl. Catal. A*, **305**, 130 (2006).
14. J.N. Yao, K. Hashimoto and A. Fujishima, *Nature*, **355**, 624 (1992).
15. Y.A. Yang, Y.W. Cao, B.H. Loo and J.N. Yao, *J. Phys. Chem. B*, **102**, 9392 (1998).
16. D. Manno, M.D. Giulio and A. Serra, *J. Phys. D*, **35**, 228 (2002).
17. J.F. Colin, V. Prolong, M. Hervieu, V. Caignaert and B. Raveau, *Chem. Mater.*, **20**, 1534 (2008).
18. X. Sha, L. Chen, C.C. Alan, P.P. Guido and H. Cheng, *J. Phys. Chem. C*, **113**, 11399 (2009).
19. R.P. Greta, M. Alexej, K. Frank, N. Reinhard, J. Grunwaldt and A. Baiker, *Chem. Mater.*, **16**, 1126 (2004).
20. S. Hu and X. Wang, *J. Am. Chem. Soc.*, **130**, 8126 (2008).
21. L. Zheng, Y. Xu, D. Jin and Y. Xie, *Chem. Mater.*, **21**, 5681 (2009).
22. X. Chen, W. Lei, D. Liu, J. Hao, Q. Cui and G. Zou, *J. Phys. Chem. C*, **113**, 21582 (2009).
23. T. Liu, Y. Xie and B.Chu, *Langmuir*, **16**, 9015 (2000).
24. L. Cai, P.M. Rao and X. Zheng, *Nano Lett.*, **11**, 872 (2011).
25. D.M. Antonelli and M. Trudeau, *Angew. Chem. Int. Ed.*, **38**, 1471 (1999).
26. G. Mestl, P. Ruiz, B. Delmon and H. Knozinger, *J. Phys. Chem.*, **98**, 11269 (1994).